Research Article

Lubrication in Aqueous Solutions Using Cationic Surfactants – a Study of Static and Dynamic Forces

K. Boschkova, B. Kronberg, J. J. R. Stlgren, K. Persson, and M. Ratoi Salagean

Langmuir, **2002**, 18 (5), 1680-1687• DOI: 10.1021/la0114676 • Publication Date (Web): 01 February 2002

Lubrication in Aqueous Solutions Using Cationic Surfactants − a Study of Static and Dynamic Forces

K. Boschkova,*[,†,‡] B. Kronberg,[‡] J. J. R. Stålgren,[†] K. Persson,[‡] and M. Ratoi Salagean[§]

Department of Chemistry, Surface Chemistry, Royal Institute of Technology, Drottning Kristinas väg 51, SE−100 44 Stockholm, Sweden, YKI, Institute for Surface Chemistry, Box 5607, SE−114 86 Stockholm, Sweden, and Tribology Section, Department of Mechanical Engineering, Imperial College of Science, Technology and Medicine, London SW7 2BX, U.K.

Received September 24, 2001. In Final Form: November 26, 2001

This paper concerns lubrication in aqueous surfactant systems where the surfactants adsorb at surfaces, in relative motion, forming either a surfactant monolayer or a multi-(liquid crystalline) layer. The surfactants were of two kinds, viz., a double chain cationic surfactant, didodecyldimethylammonium bromide, DDAB, and a single chain cationic surfactant, dodecyltrimethylammonium bromide, DTAB. Excellent film forming capability was shown for DDAB and interpreted as the result of good packing of the surfactant molecules at the surfaces, i.e., the inherent ability of the surfactant molecules to form liquid crystalline structures at the surface, resulting in good load-carrying capability. This is also reflected in the bulk properties of the surfactants, where DDAB show lamellar liquid crystalline phases at concentrations much lower than DTAB, which does not show good lubrication properties. The results are discussed in terms of film stability of a surfactant layer adsorbed at the surface, which in turn is correlated to the critical packing parameter of the surfactant, in analogy with the Kabalnov−Wennerström theory of emulsion droplet coalescence (Kabalnov, A.; Wennerström, H. *Langmuir* **1996**, *12*, 276). The systems were characterized using (i) the surface force apparatus determining the interaction forces between the adsorbed layers at the surfaces and (ii) the EHD rig (elastohydrodynamic rig) determining film formation under shear. The adsorption kinetics and composition at the surface were determined by a quartz crystal microbalance and X-ray photoelectron spectroscopy.

Introduction

The aim of the present work is to assess lubrication properties of binary water/surfactant solutions. Of special interest is the ability of various surfactant mesophases, such as lyotropic lamellar liquid crystalline structures, to act as lubricating entities. The structure of a lamellar liquid crystal is similar to that of graphite in the sense that the binding between the lamellae is weak compared to the binding between the atoms, or molecules, in the lamellae. In lamellar liquid crystalline phases, the sliding movement is therefore expected to occur between the layers. When these phases are present at the surfaces they should provide a good lubrication medium, giving a low friction coefficient.[1]

Specifically the objective of this study is to (i) investigate the importance of the inherent ability of surfactants to form liquid crystalline structures for the lubrication properties and (ii) study the effect of surfactant molecular packing at the surface. The first objective is accomplished by comparison of a single and double chain surfactant, as the double-chain surfactant is more prone to form liquid crystalline structures as reflected in the higher critical packing parameter, CPP, value.[2] Varying the proportion of single and double chain surfactant at the surfaces accomplishes the second objective. The surfactants used were the single chain dodecyltrimethylammonium bromide (DTAB) surfactant and the doubled chained analogue didodecyldimethylammonium bromide (DDAB). These surfactants were chosen since they have an affinity for the anionic surfaces used in this model study. We note in passing that it is not a necessary requirement that a lamellar liquid crystalline phase is present in the bulk liquid when testing for lubricity. It has previously been shown that a surface itself induces the formation of associated structures.[3] It is therefore sufficient that the system is prone to form lamellar structures, which in turn are induced at the surface. A prerequisite is therefore that the surfactant adsorbs at the surface in question. This is the reason for choosing cationic surfactants. Thus, in this study mixtures of a single-chain surfactant and a double-chain cationic surfactant were characterized employing several different surface sensitive techniques both under static and dynamic conditions. The static interaction forces were studied using the SFA (surface forces apparatus), and the dynamic shear properties were characterized using the EHD (elastohydrodynamic) rig. The scope was to compare the film forming ability under static and dynamic conditions. Furthermore, the systems were characterized by employing a quartz crystal microbalance, QCM to monitor the adsorption kinetics at hydrophilic gold surfaces and XPS (X-ray photoelectron spectroscopy), to determine the surfactant composition at the mica surface. Furthermore, to check the credibility of the composition determined using the carbon signal from the XPS results (due to the possibility of contaminations), both the adsorbed amount and overlayer thickness were determined from the XPS results and compared with the SFA results.

[†] Royal Institute of Technology.
[‡] YKI, Institute for Surface Chemistry.
[§] Imperial College.

(1) Friberg, S. E.; Ma, Z. *Adv. Colloid Interface Sci.* **1992**, *41*, 45.
(2) Israelachvili, J. N.; Mitchell, D. J.; Ninham, B. W. *J. Chem. Soc., Faraday Trans. 1* **1976**, *72*, 1525.
(3) Petrov, P.; Olsson, U.; Christenson, H.; Miklavic, S.; Wennerström, H. *Langmuir* **1994**, *10*, 988.

10.1021/la0114676 CCC: $22.00
Published on Web 02/01/2002

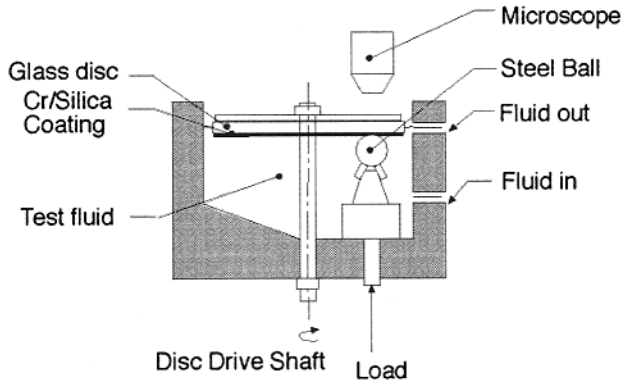

Figure 1. Schematic representation of the EHD rig.

Experimental Section

Materials. The didodecyldimethylammonium bromide (DDAB) and dodecyltrimethylammonium bromide (DTAB) (>99%) were both obtained from Sigma-Aldrich Sweden AB and was used as received.

The water used in the experiments was treated by a Milli-RO 10 Plus pretreatment unit, including depth filtration, carbon adsorption, and decalcination preceding reverse osmosis. This treatment was followed by a Milli-Q plus185 unit, which treats the water with UV light (185 + 254 nm) before a Q-PAK unit consisting of an activated carbon unit followed by mixed bed ion exchanger and finally an Organex cartridge. The outgoing water is filtered through a 0.2 μm filter.

The glue for attaching the mica sheets in the SFA (see below) was an epoxy resin (Epon 1004), supplied by Shell Chemicals.

Surface Forces Experiments. The force acting between adsorbed surfactant films at mica surfaces as a function of their separation was measured using the interferometric surface forces apparatus, SFA Mark III. A detailed description of the technique is described elsewhere.[4] The separation of the surfaces can be determined with a resolution of approximately 1−2 Å by analysis of the fringes of equal chromatic order, FECO, in the spectrometer. The interaction forces are determined by measuring the deflection of the spring onto which the lower surface is mounted, using a spring-constant, k, of 150 N/m.

Elastohydrodynamic Film-Thickness Measurements. In the elastohydrodynamic rig (EHD rig) a stainless steel ball is rolled against a transparent glass disk, and an ultrathin film technique is used to measure the separating film thickness between the ball and the disk; see Figure 1. The technique has been described in detail elsewhere.[5]

The refractive index of the lubricating liquid is a necessary input in the calculation of the film thickness. The variation of the refractive index n as a function of the volume fraction of water Θ_w of a lamellar phase has been shown to have a linear decrease with dilution.[6] The variation was found to be linear according to $n = (n_1 - n_0)\Theta_w + n_0$. Extrapolated values of the refractive index ranges from $n_0 = 1.645$ with no dilution $\Theta_w = 0$, to $n_1 = 1.334$ at $\Theta_w = 1$. In this study, the change in refractive index arising from ordering effects should not overestimate the film thickness by more than 15%, where the refractive index used for these calculations was 1.4.

The EHD film thickness measurements were performed on two separate instruments. One using fully flooded conditions and in the other, the test liquid was added to the contact by a pipet during the measurement. When the fully flooded rig was used, the solutions were left to equilibrate for at least 1.5 h before the experiment was run, unless otherwise stated. All measurements were carried out under pure rolling conditions at a contact pressure of 0.52 GPa at 27 °C.

The glassware and pieces of the apparatus coming in contact with the test solution were cleaned with 2-propanol. Before the first measurement, toluene was used prior to 2-propanol.

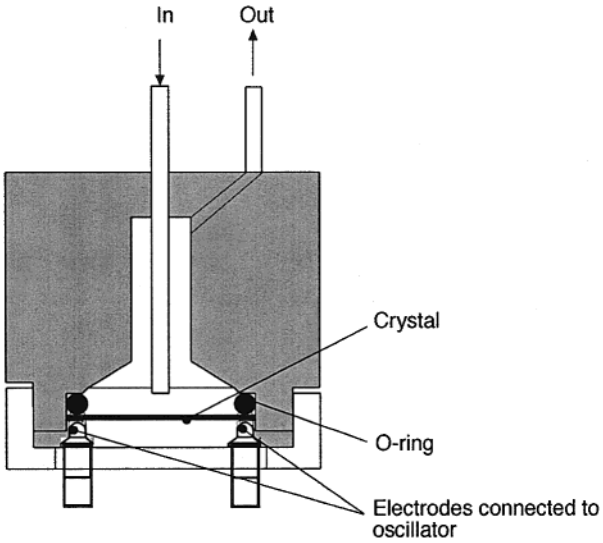

Figure 2. Schematic representation of the QCM.

Quartz Crystal Microbalance. In the quartz crystal microbalance, QCM, technique a quartz crystal is subjected to oscillations at variable frequencies and the resonance frequency is determined. This resonance frequency is proportional to the total mass of the crystal, i.e., including the adsorbed layer, according to the Sauerbrey relation (eq 1).[7]

$$\Delta m = -C\frac{\Delta f}{n} \quad (1)$$

Here, Δm is the adsorbed mass, C is a constant characteristic of the crystal, in this case, 0.178 mg/m^2 Hz, Δf is the change in frequency, and n is the shear wavenumber. This relation rests on the assumption that the deposited mass forms a thin rigid film and that the mass sensitivity is uniform over the entire surface. Equation 1 has been supported by experimental data up to mass loadings of approximately 2% of the mass of the crystal itself.[8] There are various models for converting the frequency shift to adsorbed mass. However, these models give identical adsorbed amount for a given frequency up to approximately 5% of mass loading.[9]

The quartz crystal microbalance used here is a QCM-D from Q-sense, Gothenburg, Sweden; see Figure 2. The fluid cell is temperature controlled to 25 ± 0.02 °C. The technique allows for simultaneous measurement of changes in resonance frequency and energy dissipation, where the dissipation is a measure of the viscoelastic properties of the adsorbed layer.

The surfaces used for these experiments where gold surfaces with a 3D surface roughness of 2 ± 0.2 nm (measurement area: 0.18 mm × 0.13 mm), determined using a profilometer, Zygo View 5010. The QCM cell and the tubing were cleaned using a 2% Hellmanex II solution for 1 h. The system was then rinsed with water and the crystal was also dismounted and cleaned with ethanol. The system was thereafter rinsed with excess water while monitoring the frequency and dissipation values. The injection time was kept constant at approximately 90 s and at each injection 1.5 mL of surfactant solution was supplied to the cell. In total, three injections were made to saturate the surface with surfactant, thereby eliminating depletion effects.

Determination of Surface Composition. It is essential to know the surface composition in these experiments since it could adversely differ from the bulk composition, i.e., the original composition of the solution. The surface composition was calculated using the ideal solution model and also determined by XPS. The total surfactant concentration was kept constant at 0.3 × cmc when not stated otherwise. Here cmc represents the critical micelle concentration of the mixed surfactant system. The cmc for a mixed surfactant system was calculated using

(4) Luengo, G.; Schmitt, F. J.; Hill, R.; Israelachvili, J. *Macromolecules* **1997**, *30*, 2482.
(5) Johnston, G. J.; Wayte, R.; Spikes, H. A. *Tribol. Trans.* **1991**, *34*, 187.
(6) Gomati, R.; Gharbia, M.; Gharbi, A. *Opt. Commun.* **1994**, *111*, 71.
(7) Sauerbrey, G. *Z. Phys.* **1959**, *155*, 206.
(8) Pulker, H. K. *Z. Angew. Phys.* **1966**, *20*, 537.
(9) Mecea, V.; Bucur, R. V. *Thin Solid Films* **1979**, *60*, 73−84.

Table 1. Total Surfactant Composition, x_{DTAB}, Micellar and Surface Composition, $x^{s,m}_{DTAB}$, and Surfactant Solution Concentration, *c*, for the Different Micellar and Surface Compositions of 0.3 × Cmc DDAB and DTAB[a]

x_{DTAB}	$x^{s,m}_{DTAB}$ (theor)	*c*, DDAB (μM)	*c*, DTAB (mM)	cmc (mM)	x^{s}_{DTAB} (exptl)
0	0	24.0		0.08	
0.987	0.3	16.8	1.3	4.40	0.25
0.994	0.5	12.0	2.2	7.30	0.45
1.000	1.0		4.4	15	

[a] Results from XPS measurements on 0.3 × cmc solutions with different compositions. The experimental composition is calculated from the total number of C atoms.

ideal mixing theories.[10] In this model, the regular solution approach is used for description of the mixing of two surfactants in a micelle. In our system, the two surfactant types have the same type of headgroup, and it is therefore reasonable to assume zero net interaction between the two surfactants. The expression for the cmc of a mixture then has the following form (eq 2):

$$\frac{1}{\mathrm{cmc}} = \frac{x_{DTAB}}{\mathrm{cmc}_{DTAB}} + \frac{x_{DDAB}}{\mathrm{cmc}_{DDAB}} \quad (2)$$

Here cmc_{DTAB} and cmc_{DDAB} are the cmc's for the neat surfactants, while cmc is the critical micelle concentration of the mixture. The x_{DTAB} and x_{DDAB} are the bulk, or total composition, of the two surfactants, viz. (eq 3)

$$x_{DTAB} = \frac{C_{DTAB}}{C_{DDAB} + C_{DTAB}} \quad (3)$$

where C_{DTAB} and C_{DDAB} are the surfactant molar concentration in solution.

In this work, we are interested in the molar composition at the surface, which is assumed to be the same as the molar composition in the mixed micelle. It has previously been shown that the surfactant composition at a surface can be approximated to be the same as the micellar composition,[11] x^{m}_{DTAB}, especially when the cmc's of the two surfactants differ by some orders of magnitude as in our system. This is expressed as (eq 4)

$$x^{m}_{DTAB} = \frac{x_{DTAB}\mathrm{cmc}_{DDAB}}{x_{DTAB}\mathrm{cmc}_{DDAB} + (1 - x_{DTAB})\mathrm{cmc}_{DTAB}} \quad (4)$$

From inspection of the formula, it is realized that the surface composition changes dramatically with solution composition if the ratio of the surfactant cmc's is far from unity, i.e., if the two surfactants differ very much in their hydrophobicity. This implies that a small addition of a hydrophobic surfactant changes the surface composition dramatically. Such is the case in this study where the more hydrophilic surfactant (DTAB) has a cmc of 15 mM[12] while the hydrophobic, double chain surfactant (DDAB) has a cmc of only 0.08 mM.[13] Hence eq 4 predicts a preferential adsorption of DDAB compared to that of DTAB.

Using eqs 3 and 4, the cmc for the surfactant mixtures were calculated. For example the cmc of a micellar mixture (when $x^{m}_{DTAB} = 0.3$) is 4.4 mM and the mole fraction in solution is, $x_{DTAB} = 0.987$, as shown in Table 1. The actual concentrations for the different micellar compositions of DDAB and DTAB and the new cmc are listed. In the following sections only the micellar or surface compositions, x^{s}_{DTAB}, are displayed.

X-ray photoelectron spectroscopy was used to measure the surface composition in order to verify the calculations above. The basic principles of the technique have been described elsewhere.[14] Mica surfaces with the size of 2 × 3 cm were immersed in a surfactant solution for 24 h. To avoid surfactant deposition upon withdrawal from the liquid to the air interface, the solution was then diluted by a factor of ca. 30 and the surfaces were withdrawn from the solution and blow-dried with nitrogen air before being analyzed in the X-ray photelectron spectrometer, (Kratos analytical, AXIS-HS).

Herder et al.[15] previously described the quantitative determination of the surface composition of adsorbed mixed surfactants using XPS. In this model, it is assumed that the surfactants adsorb homogeneously with the polar group oriented toward the mica surface. The adsorbed amount was quantified from the N 1s/K 2s XPS signal. When small amounts are detected, plasmons can contribute to the signal, which has been accounted for in the analysis of the peak area.

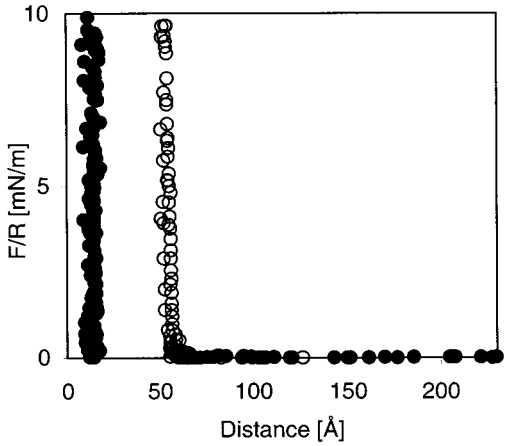

Figure 3. Force normalized by radius as a function of surface separation between mica surfaces across 0.3 × cmc DTAB (filled circles) and 0.3 × cmc DDAB (unfilled circles). Forces are measured on approach.

Results

Normal Force Measurements Using the SFA. When measuring normal forces, it was found that the adsorption process was in general slow; e.g., DDAB formed a monolayer after 1−2 h of adsorption, and after approximately 7−8 h, a double layer was formed. Normal forces between two mica sheets in aqueous solution of DDAB and DTAB are illustrated in Figure 3. The double chain surfactant, DDAB ($x^{s}_{DTAB} = 0$) apparently forms a bilayer structure at each mica surface, with a thickness of 30 Å, which is consistent with previous studies.[16,17] The single-chain surfactant, DTAB ($x^{s}_{DTAB} = 1$) displays a force barrier at approximately 15 Å thickness, indicating a flat configuration of the adsorbed molecules (a fully extended C_{12} alkyl chain length is about 17 Å). The flat configuration is consistent with SANS measurements at 40 °C, where DTAB forms oblate ellipsoid structures with half axes $a = 9$ Å and $b = 20$ Å at cmc.[18] The absence of double layer forces at large distances indicate that the adsorbed DDA^{+} and DTA^{+} ions almost completely neutralize the charges on the mica surfaces. There is only a slight build up of a second layer of DTAB ions onto the hydrophobic monolayer, which is easily pushed out from the surface at a separation of ca. 55 Å. This is a slightly thicker layer than previous observations,[19] where an

(10) Rubingh, D. N. *Solution chemistry of surfactants*; Mittal, K. L., Ed.; 1979; Vol. 1, Mixed micelle solutions, p 337.
(11) Kronberg, B.; Lindström, M.; Stenius, P. *ACS Symp. Ser.* **1986**, *311*.
(12) Evans, D. F.; Allen, M.; Ninham, B. W.; Fouda, A. *J. Solution Chem.* **1984**, *88*, 5084.
(13) Ricoul, F.; Dubois, M.; Zemb, T.; Plusquellec, D. *D., Eur. Phys. J., B* **1998**, 333.
(14) Siegbahn, K. *Science* **1982**, *217*, 111.
(15) Herder, P. C.; Claesson, P. M.; Herder, C. E. *J. Colloid Interface Sci.* **1987**, *119*, 155.
(16) Pashley, R. M.; McGuiggan, P. M.; Ninham, B. W.; Brady, J.; Evans, D. F. *J Phys. Chem.* **1986**, *90*, 1637.
(17) Manne, S.; Gaub, H. E. *Science* **1995**, *270*, 1480.
(18) Bergström, M.; Pedersen, J. S. *Phys. Chem. Chem. Phys.* **1999**, *1*, 4437.

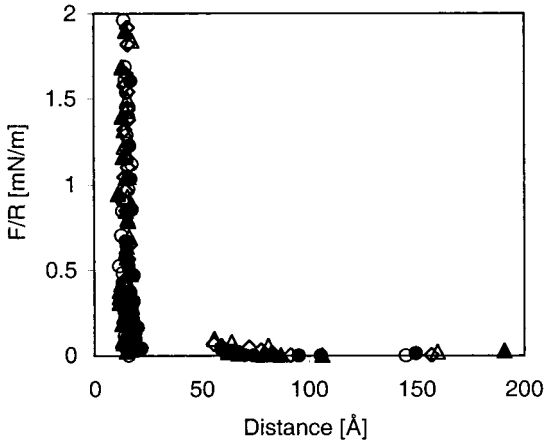

Figure 4. Force normalized by radius as a function of surface separation between mica surfaces across 0.3 × cmc, $x^s_{DTAB} = 0.3$ (unfilled circles), and 0.3 × cmc, $x^s_{DTAB} = 0.5$ (filled circles). Forces are measured on approach.

Table 2. Film Thickness, *h*, Results from SFA Measurements for the Different Micellar Compositions at 0.3 × Cmc

x^s_{DTAB}	*h* (Å)
0	60
0.3	15
0.5	15
1.0	15

average spacing between cylindrical micelles of DTAB onto mica has been determined from AFM imaging to be 48 ± 2 Å.

Surface forces measurements on mixed DDAB and DTAB surfactants were also performed. The results for $x^s_{DTAB} = 0.3$ and $x^s_{DTAB} = 0.5$ are shown in Figure 4 and display an almost identical behavior in that the force curves compared to the single DTAB surfactant, $x^s_{DTAB} = 1$. Here there is a weak barrier at ca. 60 Å that is easily collapsed upon pressure into a strong barrier at ca. 15 Å. The results are summarized in Table 2.

Thickness Measurements from Fully Flooded EHD Film. The film thickness was monitored at different speeds under pure rolling condition. In Figure 5, 0.15 × cmc DDAB ($x^s_{DTAB} = 0$) is compared with 1.5 × cmc DTAB ($x^s_{DTAB} = 1$). It is seen that DDAB gives much larger film thickness than DTAB, even though the DDAB system is far below its cmc and the DTAB is above its cmc. It was impossible to run solutions of 0.15 × cmc of DTAB since these caused high wear of the disk. Results from the mixed system (not shown) at 0.3 × cmc, $x^s_{DTAB} = 0.3$, gave better operating performance than the single chain surfactant at low speeds. However, the system was very unstable at speeds above 0.07 m/s. At 0.06 m/s, the system, 0.3 × cmc, $x^s_{DTAB} = 0.3$, forms a 60−120 Å thick film, and it is very sensitive to shear history. In general, all measurements where extremely shear sensitive. For example, for 0.15 × cmc DDAB, the film thickness shifts from 400 Å at 2 m/s in the first approach, with no equilibration time after applying the test solution (not shown) to 600 Å at 2 m/s in the second approach (Figure 5), with 2 h of equilibration. At low shearing speeds, i.e., below 0.25 m/s, however, the same thickness was detected, i.e., irrespective of equilibration time.

There are in general three features of the film thickness results. Initially there is a region where the film thickness increases with rolling speed reaching a plateau with almost constant film thickness, and then, at a critical rolling speed, the film thickness follow the EHD theory for water; i.e., it increases with rolling speed. The central film thickness was calculated for the elastic-isoviscous lubrication regime using the Hooke equation[20] (eq 5), displayed as a solid line in Figure 5

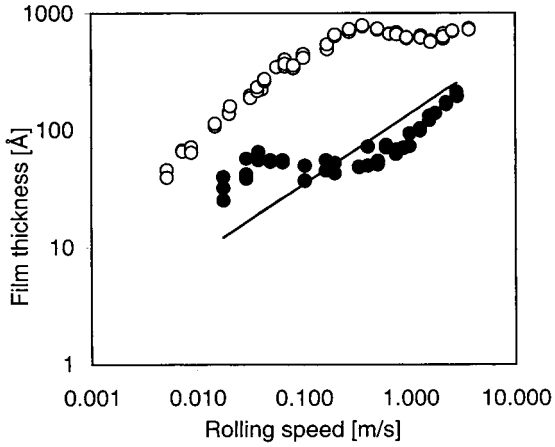

Figure 5. Results from the fully flooded EHD rig. Film thickness vs rolling speed for solutions of 0.15 × cmc DDAB (unfilled circles) and 1.5 × cmc DTAB (filled circles), respectively. The central film thickness of water was calculated for the elastic-isoviscous lubrication regime using the Hooke equation (eq 11) and displayed as a solid line.

$$h = 4.177\frac{(U\eta_0)^{0.6}R'^{2/3}}{E'^{7/15}W^{2/15}} \quad (5)$$

where *h* is given in m, *U* is the rolling speed in m/s, η_0 is the absolute viscosity of water, $\eta_0 = 0.001$ Ns/m^2, R' is the radius of the ball, $R' = 0.0095$ m, and E' is the reduced Young's modulus of the two contacting solids defined by $E' = 2((1 - \nu_1^2)/E_1 + (1 - \nu_2^2)/E_2)$, where ν_i is Poisson's ratio for material *i* and E_i is the elasticity modulus of material *i*, $E' = 1.17\text{E} + 11$ Pa, and *W* is the applied load, where $W = 20$ N.

If the above given values are inserted, the expression can be simplified to (eq 6)

$$h = 1.36U^{0.6} \times 10^{-8}\ \text{m} \quad (6)$$

During the initial stage the surfactants tend to organize (possibly into well aligned lamellar sheets) during shear, and this is clearly seen for the DDAB system. The initial reorganization for DTAB is much less pronounced which indicates a more disordered structure with poor film forming properties and results in a thinner film.

The film formation of DTAB and the mixed component system is similar to monolayer (bilayer) boundary single chain surfactant films observed by Ratoi and Spikes.[21] It is concluded that the stiffer doubled chain surfactant favors an ordered structure with much better film forming properties than the single chain surfactant.

Thickness Measurements from Non-Fully-Flooded EHD. In Figure 6 the relaxation behavior after shearing is shown, where the film thickness is plotted vs time after the shear has stopped. It is seen that after relaxation the film thickness given in Table 3 is close to the static values given by the surface forces measurements (Table 2), despite the different nature of the surfaces.

(19) Patrick, H. N.; Warr, G. G.; Manne, S.; Aksay, I. A. *Langmuir* **1999**, *15*, 1685.

(20) Hooke, C. J. *J. Mech. Eng. Sci.* **1980**, *22*, 183.

(21) Ratoi, M.; Spikes, H. A. *Tribol. Trans.* **1999**, *42*, 479.

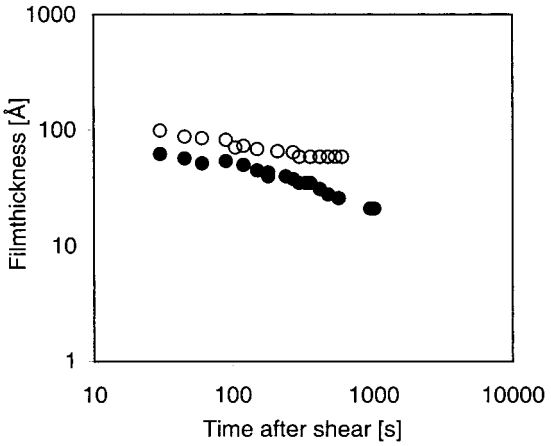

Figure 6. Relaxation experiment in the nonfully flooded EHD rig. Film thickness vs time for solutions of 0.15 × cmc DDAB (unfilled circles) and 0.3 × cmc, $x^s_{DTAB} = 0.3$ (filled circles), after stopping shear.

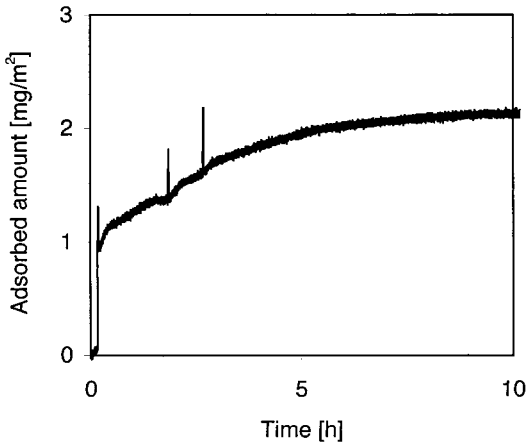

Figure 7. Adsorption kinetics for 0.3 × cmc DTAB onto a gold surface. The solution is exchanged after 1.5 and 2.5 h after the first injection.

Table 3. Static Film Thickness, *h*, after EHD Relaxation Measurements on 0.15 × Cmc, $x^s_{DTAB} = 0$, and 0.3 × Cmc, $x^s_{DTAB} = 0.3$, at Equilibrium

x^s_{DTAB}	*h* (Å)
0	59
0.3	20

Adsorption Kinetics Determined from the QCM Technique. Both the fundamental resonance frequency and the third overtone, which is more surface sensitive, were monitored during the adsorption process. In these experiments, it was observed that the fundamental frequency was less reproducible than the signal from the third overtone. It was also observed that the signal obtained from the fundamental frequency was very sensitive to surfactant concentration and history of the sample.

QCM measurements where performed on DDAB, DTAB and solutions of mixtures thereof. By using the Sauerbrey relation, the adsorbed amount was calculated from the third overtone. The adsorption kinetics of the single surfactant system 0.3 × cmc of DTAB, ($x^s_{DTAB} = 1$) and the mixed surfactant system 0.3 × cmc, $x^s_{DTAB} = 0.5$ are displayed in Figures 7 and 8.

The figures reveal that the build up time of the film is very different between the single and mixed surfactant systems. The two single surfactant systems both attain

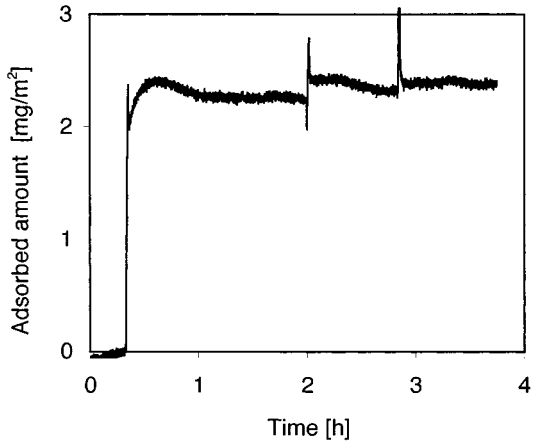

Figure 8. Adsorption kinetics for 0.3 × cmc, $x^s_{DTAB} = 0.5$, onto a gold surface. The solution is exchanged after 1.5 and 2.5 h after the first injection.

Table 4. Mean Values of Results from QCM Measurements on 0.3 × Cmc Solutions of DDAB and DTAB[a]

x^s_{DTAB}	*A* (Å²)	*T* (h)
0	50	≈8
0.5	60	≈1
1	50	≈8

[a] The area per molecule, *A*, is calculated from the number density values (from the frequency shift) at the adsorption plateau (assuming a bilayer adsorption model). The time for reaching the adsorption plateau is also given.

90% of the adsorption plateau after approximately 8 h of adsorption, displayed for 0.3 × cmc DTAB in Figure 7, whereas the mixed surfactant system reach approximately 90% of the adsorption plateau after ca. 40 min of adsorption time; see Figure 8.

From the adsorbed amount the area per molecule, *A*, of the surfactants was calculated using a mean value of two independent measurements. In these calculations we used the ideal mixing model for calculating the surfactant composition at the surface. It was assumed that the counterion, Br^-, is incorporated within the adsorbed structure. The surfactant molecular area and adsorption time for reaching the adsorption plateau (as estimated from Figures 7 and 8) are shown in Table 4. It is observed that all systems display a similar behavior, i.e., an occupied area between 50 and 60 Å² per molecule, irrespective of surfactant assuming a bilayer adsorption.

Determination of the Surface Composition Using XPS. To verify the calculated surface composition with respect to the surfactants (eq 4), we used the methodology using XPS as developed by Herder et al.[15] The quantification is determined from the number of adsorbed carbon molecules $N_M(C)$, per unit area, *A*, according to (eq 7)

$$\frac{N_M(C)}{A} = \frac{I_C S_K (d/(\lambda_L \sin \Theta))}{I_K S_C \mathrm{FR}[\exp(d/(\lambda_L \sin \Theta) - 1]} \times 2.1 \times 10^{14} \quad (7)$$

where I_C and I_K represent the measured peak intensity for carbon and potassium, S_K and S_C are the sensitivity factors for the potassium and carbon signals due to the adsorbed layer with a thickness, *d*, onto the mica, λ_L is the inelastic mean free path, and Θ is the photoelectron takeoff angle.[15] FR is the signal emanating from the exchangeable potassium ions at the surface, divided by the signal from

Table 5. Results from XPS Measurements on 0.3 × Cmc Solutions of DDAB and DTAB[a]

x^s_{DTAB}	$N \times 10^{18}$ (m^{-2})	a ($Å^2$)
0	1.84	54
0.3	1.93	52
0.5	1.85	55
1.0	1.78	56

[a] The number density, N, is calculated using eq 5. The area per molecule, A, is calculated from the number density assuming a monolayer adsorption.

potassium ions situated in the bulk below the mica surface and experimentally determined to be equal to 0.1971.

From the number of adsorbed atoms per unit area the composition was calculated using the following formula (eq 8):

$$\alpha N_A^{DDAB} + (1 - \alpha)N_A^{DTAB} = N_A^{Mixed} \quad (8)$$

The average surface compositions, with respect to the surfactants, are given in Table 1.

Determination of Adsorbed Amount by Using XPS. The XPS results can also be used to calculate the adsorbed amount of surfactant at the mica surface. Quantification based on the nitrogen signal was calculated using eq 5. A mean value of two measurements of the number of adsorbed nitrogen molecules, $N_M(N)$ per unit area, A, are displayed in Table 5. It is observed that the total adsorbed amount is almost the same irrespective of surfactant composition. The number of adsorbed molecules was calculated from[15] (eq 9)

$$\frac{N_M(N)}{A} = \frac{I_N S_K}{\bar{I}_K S_N (FR)}(2.1 \times 10^{14}) \quad (9)$$

with the same notation used as for eq 8. Furthermore, $\bar{I}_K$ is the reduction of the potassium signal due to the adsorbed layer with a thickness, d, onto the mica and described by (eq 10)

$$\bar{I}_K = I_K \exp(-d/(\lambda_L \sin \Theta)) \quad (10)$$

where λ_L is the inelastic mean free path and Θ is the photoelectron takeoff angle.[22]

Using the number density, $N_M(N)/A$, the area per molecule was calculated for all surfactant combinations giving a value between 52 and 56 $Å^2$, as displayed in Table 5.

Determination of the Overlayer Thickness Using XPS. The overlayer thickness was determined by measuring the photoelectron emission, I, upon varying the photoelectron takeoff angle, Θ. Determining the slope from ln I plotted against sin(Θ) represents the reduced thickness, t_0/λ_0. The film-thickness is then calculated by multiplying the slope, k, with the IMFP, inelastic mean free path (eq 11)

$$t_0 = k\lambda_a^0 \quad (11)$$

where the IMFP can be calculated from the following relation[23] (eq 12):

$$\lambda_a^0 = \frac{M}{\rho N_v} E_a / [13.6 \ln(E_a) - 17.6 - 2100/E_a] \quad (12)$$

where M is molecular weight, ρ is the density (g cm^{-3}), N_v is the number of valence electrons per molecule, and E_a is the kinetic energy of the ejected photoelectron (eV). The value of λ_a^0 is given in angstrom units (Å).

The slope, k, is determined from a linear fit of ln I vs sin(Θ), where intensity values from four different angles, 15, 20, 30, and 45°, were used. A linear fit with a correlation better than 0.94 was obtained for all samples.

The surfactant layer thickness, t_0, at the mica surface, determined from the K 2p and K 2s XPS signals was found to be 20−30 Å for DDAB and 14−20 Å for DTAB as displayed in Table 6. Both the K 2p and the K 2s signal indicate that DDAB forms a thicker film than DTAB, consistent with the surface forces experiments.

Discussion

The double chain surfactant, DDAB, is more prone to form a compression-resistant structure compared to the single chain surfactant, DTAB, as seen from the surface forces experiments, showing that it forms a bilayer at each mica surface. The total thickness between the mica sheets is 60 Å. The single chain surfactant and the mixed surfactant system build up a film of approximately 8 Å thickness at each surface indicating a more patchwise or flat configuration at the surface. The results from the mixed surfactant systems indicate that the DTAB is very efficient in destroying the lamellar structure of DDAB. Thus, even when present in as small relative amount as 30% (mole fraction) at the surface, the system behaves almost as if it would entirely be made up of DTAB. This is remarkable since the DTAB is the less surface active component, and hence the surface should be dominated by the properties of DDAB. We conclude that the DTAB is very efficient in reducing the critical packing parameter of the DDAB adsorbed at the surface, resulting in the surface forces shown.

The results from the EHD runs (Figures 7 and 8) show that both the DDAB and DTAB surfactants form much thicker films under dynamic shearing conditions compared to static conditions. A solution of 0.15 × cmc DDAB forms films with a thickness of 600−800 Å at rolling speeds above 0.1 m/s, whereas a solution of 1.5 × cmc DTAB forms films that are 60−80 Å thick, at rolling speeds above 0.01 m/s. However, above 1 m/s, the system displays the same properties as water. It is thus evident that the DDAB surfactant forms an induced structure during shear, with good load-carrying capabilities. The structure also relaxes into the original state approximately 10−15 min after the shear has been stopped. This implies that the new structures formed under shear are not permanent. Interestingly the thickness of the static film is similar in the SFA and EHD rig, despite the different surfaces and surface roughness. It is thus clear that an organized structure is built up by shear, and it gradually relaxes when the shear has stopped. Most probably a close packed lamellar structure is formed. By disturbing the structure on addition of DTAB to DDAB the structure changes and the load-carrying capability decreases.

The slow adsorption process is monitored using the QCM. The mixed surfactant systems display faster adsorption times, i.e., 1 h for the mixed systems and approximately 8 h for the single component system. The large difference in adsorption time between single and mixed surfactant systems can be understood considering that the total surfactant concentration, in the bulk

(22) Briggs, D.; Seah, M. P. *Practical surface analysis*, 2nd ed.; Wiley: Chichester, England, 1990; Vol. 1.
(23) Ashley, J. *J. Electron Spectrosc. Relat. Phenom.* **1982**, *28*, 177.

Table 6. Thickness Determination from K 2s and K 2p XPS Signals of 0.3 Cmc DDAB and DTAB on Mica

x^s_{DTAB}	$\lambda^0_{K\,2s}$ (Å)	$\lambda^0_{K\,2p}$ (Å)	k	t_0(K 2s) (Å)	t_0(K 2p) (Å)
0	41.07	43.51	0.53	21	29
1.0	41.06	43.50	0.52	14	23

[a] $\lambda^0_{K\,2s}$ and $\lambda^0_{K\,2p}$ are the photoelectron inelastic mean free paths, IMPF, for peaks K 2s and K 2p. k, is determined from the slope of ln(I) vs sin Θ, t_0(K 2s) and t_0(K 2p) is the overlayer thickness determined from the K 2s and K 2p signal.

solution, in all cases is far below the cmc. Since the adsorption of surfactants behave approximately the same if plotted as a function of the reduced concentration, viz. the concentration divided by the cmc of the solution, we first conclude that the adsorbed amount at the surface is approximately the same, irrespective on the surfactant system. However, in the mixed surfactant systems, the chemical potential of each surfactant at the surface is lower, compared to the single surfactant systems, which is due to the entropy of mixing. There is thus a larger driving force toward the surface for the surfactants in the mixed systems and hence there should be a faster adsorption.

No conclusion can be drawn concerning the dissipation changes during the adsorption of the cationic surfactants at the QCM crystals. This might be due to the high surface roughness of the gold surface, since the surface roughness is in the same order as the extension of the surfactants. However, we note that the adsorbed amount and adsorption kinetics are consistent with the surface forces results. The area per molecule of 50−60 Å^2 is believed to correspond to a defective bilayer or micellar structure (a bilayer adsorption model is assumed).

The slow adsorption kinetics of the two single surfactants (DDAB and DTAB) is in agreement with previous observations below the cmc, it is observed that CTAB reaches 90% of its adsorption-plateau from 0.55 × cmc solution on a silica interface in 11 hours.[24] It is suggested that the adsorption rate below the cmc is limited by slow rearrangements within the layer. At low surfactant concentration, a net surface charge reversal takes place, and it is observed that the electrostatic repulsion from the interface significantly hinder the adsorption. Likewise Ducker et al. have found that CTAB's initially form a cylindrical structure onto mica and then transform into a flat sheet after 24 h.[25] This is attributed to slow exchange of potassium ions in the mica lattice for the CTA^+ molecule.

We note that the XPS measurements on mica confirm that the adsorbed amount corresponds to a surfactant cross sectional area of 52−56 Å^2, which is close to the mica lattice charge density (48 Å^2). This is consistent with the observation of absence of strong double layer forces in the surface forces experiments. Furthermore, the XPS measurements detect similiar adsorbed amounts compared to the QCM results.

We suggest viewing the results in the light of the theory of thin film stability, as proposed by Kabalnov and Wennerström[26] for the stability of emulsions. Here the authors discuss the stability of a thin oil film separating two water droplets in a water-in-oil emulsion (or conversely a thin water film separating two oil droplets in a oil-in-water emulsion). The film is stabilized by surfactants and the instability is determined by the easiness of forming a water bridge (a hole) in the oil film in the first case. Thus surfactants having a molecular structure such that a water bridge easily can be formed are poor emulsifiers, while good emulsifiers are surfactants having such a molecular structure that they prevent the formation of a bridge. The critical packing parameter, CPP as developed by Israelachvili et al.,[2] conveniently describes the surfactant molecular structure. Hence, there is a large free energy of forming a hole in the oil film if the surfactant has a high CPP. On the other hand, there is a low free energy of forming a hole if the surfactant CPP is low. Hence, the stability of the oil film increases with an increase of the surfactant's CPP.

We propose that the film formation and film stability between two solid surfaces can be viewed likewise; viz., the film formation is rendered more difficult if there is a high probability of forming a hole in the film, i.e., in systems where the CPP is low. Here, by "a hole" is meant a water bridge linking the two solid surfaces. Thus, thermal and mechanical fluctuations lead to spontaneous formation of holes, or channels of water, between the surfaces. Hence, bad film-forming properties are analogous to hole formation in the surfactant film separating the surfaces. Thus it is expected that both film-forming ability and film stability increase with increasing CPP.

The hole formation is facilitated as the CPP of the surfactant system decreases. Thus, small holes prevent structuring in layers and act as destabilizer of the lubricating surfactant film. DTAB has a lower CPP than DDAB and is therefore more prone to form small hole like structures, which will rupture the lubricating film. Similarly a mixture with $x^s_{DTAB} = 0.5$ also has a lower CPP, explaining the poor lubricating performance of this mixture.

Conclusions

We note with interest that the different surfactant systems studied display similar adsorbed amounts but different surface structures giving rise to different shearing properties and resistance against compression. Indeed, the double-chain surfactant is more prone to form liquid crystalline structures resulting in a shear induced structure of surfactant aggregates at the surface, with good load-carrying capabilities, whereas the single chain surfactant displays poor film forming properties as a result of poor structuring properties. It is proposed that the observed trends can be understood in terms of the hole theory of Kabalnov and Wennerström, created for an understanding of coalescence of emulsions. The hole formation is facilitated as the CPP of the surfactant system decreases, creating small holes that act as a destabilizer of the lubricating film. The energy of forming a hole is larger for surfactants with high CPP than for surfactants with low CPP. DDAB, which has a high CPP, is therefore more prone to form lubricating films between two shearing surfaces. Also, upon addition of single chain cationic surfactant a lubricating film cannot be formed, which is attributed to the formation of holes.

These findings have practical implication in water-based lubrication systems, which is of growing technical interest today. Water-based lubrication is of interest in applications where for example the prevention of leak oils are of concern, e.g., in food, pharmaceutical, and mining industries. In this study, it is shown that small amounts of double chain surfactant in a water solution have very promising film forming capabilities, which is attributed to the formation of a densely packed amphiphile layer. However this lubricating film is easily destroyed upon the addition of a surfactant with a low CPP.

(24) Pagac, E. S.; Prieve, D. C.; Tilton, R. D. *Langmuir* **1998**, *14*, 2333.
(25) Ducker, W. A.; Wanless, E. J. *Langmuir* **1999**, *15*, 160.
(26) Kabalnov, A.; Wennerström, H. *Langmuir* **1996**, *12*, 276.

Acknowledgment. K.B. gratefully acknowledges financial support from the Swedish Research Council for Engineering Sciences. J.J.R.S. acknowledges financial support from the SSF, Colloid and Interface Technology Program. K.P. acknowledges financial support from Vinnova. Mikael Sundin and Marie Ernstsson are acknowledged for contributions in XPS measurements.

LA0114676